The Iraqi Journal For Mechanical And Material Engineering, Vol.14, No1, 2014

# THREE DIMENSIONAL ANALYSIS OF THERMAL STRESSES AND STRAINS IN COMPOSITE EXHAUST TUBE MODEL AT DIFFERENT SALT CONCENTRATION RATIOS

**Dr. Raed Naeem Hwyyin[1]** **Lecturer Azhar Sabah Ameed[2]**
**Ass. Lect. Adnan Ghareeb Tuaamah[3]**

## ABSTRACT

The study investigates effect of salt ratio on the thermal stress and strain concentration in composite exhaust tube model. The study builds three-dimensional model of exhaust tube and analyses it numerically with finite element method using ANSYS Software. The investigation depends on the experimental results of tensile test and thermal conductivity test to determine the mechanical and thermal properties of composite specimens. The composite specimens were immersed in the salt environment of different concentration ratios (15%, 35%, and 55%) for forty days. The numerical results show that the thermal stresses ($\sigma_x$, $\sigma_y$ and $\sigma_z$) at node number (2873) increases by ratio of (58.2%) while the thermal shear stress ($\tau_{xy}$) at node number (20600) increases by approximate ratio of (56.17%) as a result of increase in the salt concentration ratio from (15%) to (55%). The maximum thermal shear strain ($\gamma_{xy}$) increases with ratio of (21.8%) due to increase in the salt concentration ratio from (15%) to (55%). The maximum thermal stresses and strains concentrate at the end of composite exhaust tube model as a result of expansion which happened in the tube model. The temperature distribution and heat transition with time is described in three dimensional composite exhaust tube model. The theoretical and numerical results are compared, and the disparity between them is equal to (9%).

**Keyword: composite material, three-dimensional analysis, conductivity, thermal stress, thermal strain and heat transition.**

# التحليل الثلاثي الابعاد للاجهادات والانفعالات الحرارية في انموذج انبوب العادم المركب عند نسب تركيز ملحي مختلفة

## الخلاصة

تبحث الدراسة الحالية في تأثير نسبة التركيز الملحي على الاجهادات والانفعالات الحرارية في انموذج انبوب العادم المركب. بنت الدراسة أنموذج ثلاثي الابعاد لانبوب العادم وتم تحليله عددياً بطريقة العناصر المحددة باستخدام برنامج الـ ( ANSYS). اعتمد البحث على النتائج العملية لاختبار الشد واختبار الموصلية الحرارية لتحديد المواصفات الميكانيكية والحرارية للعينات المركبة. غُطست العينات المركبة في محيط ملحي بنسب تركيز مختلفة (15%، 35% و 55%) لاربعين يوماً. تظهر النتائج

[1] Petroleum Technology Department - University of Technology
[2] Electromechanical Engineering Department - University of Technology
[3] Center of Training and Factory- University of Technology

العددية ان الاجهاد الحراري ($\sigma x$ , $\sigma y$ و $\sigma z$) عند عقدة رقم (2873) يزداد بنسبة (58.2%) بينما اجهاد القص الحراري ( $\tau_{xy}$) عند العقدة ( 20600) يزداد بنسبة تقريبية ( 56.17%) نتيجة لزيادة نسبة التركيز الملحي من ( 15%) الى (55%). يزداد انفعال القص الحراري الاقصى ($\gamma_{xy}$) بنسبة (21.8%) بسبب زيادة نسبة التركيز الملحي من ( 15%) الى (55%). يتركز الاجهاد والانفعال الحراري الاقصى عند نهاية أنموذج الانبوب العادم المركب نتيجة التمدد الحاصل في أنموذج الانبوب. توزيع درجات الحرارة و الحرارة المنتقلة مع الزمن وصف في أنموذج انبوب العادم ثلاثي الابعاد. النتائج النظرية والعددية تم مقارنتها والتفاوت بينهم يساوي الى (9%).

**الكلمات المرشدة: المادة المركبة، التحليل ثلاثي الابعاد، الموصلية الحرارية، الاجهاد الحراري، الانفعال الحراري و الحرارة المنتقلة**

## INTRODUCTION

Many application studies of structural materials involving composites include impact or dynamic loading in a humid environment. Composite materials are known to get damaged when subjected to humid conditions, and therefore the humidity confounds the difficulty of determining the high strain rate behavior of composites. (**Abdalla et al. 2010**) studied composites specimens containing (10%, 20%, and 30%) weight percentages of fiber. Water absorption tests were conducted by immersing these specimens in a distilled water bath at 25C$^o$ for four months. The tensile properties of the specimens immersed in water were evaluated and compared with the dry composite specimens.

Several researchers have found that water absorption by composites causes damage of matrix and dominates quasi-static properties. The study includes dry, medium, and saturated moisture conditions. The tests show significant variation in high strain rate properties from static properties, and the reasons are identified. In addition, a better understanding of the effect of the matrix and fiber/matrix interface on the high strain rate properties of composites is achieved (**Eyassu 2004**). The cross-linking reaction between unsaturated polyester resins and vinyl monomers, i.e. styrene, allows one polymer chain to connect with other polymer chains to produce a three dimensional network, which converts the resin system from a viscous liquid into a hard, thermoset solid, (**Radoljub P. Tomi et al 2011**). The finite element analysis (FEA) approach is utilized to perform heat transfer analysis and to obtain steady state temperature distribution from the steam-line (process pipe) surface along the stanchion toward the end plate. Multipurpose finite element program ANSYS is utilized in this study. (**Chakrapani Basavaraju, 2004** ) The steady state temperature distribution addressed in this paper is not applicable to transients, such as short heat-ups or cool-downs, for which a transient analysis is required. Heat transferred from the insulated steam process pipe is through conduction into the stanchion for the 5.5” length portion covered with the process pipe insulation, and then by conduction and convection mechanisms to the uninsulated portion of the stanchion and end plate welded to the stanchion and exposed to the surrounding air at 70 to 100°F. The process pipe steam temperatures considered are 800$^o$F,and 1013$^o$F .

(**G. Anagnostopoulos et al 2007**) made a study on the thermal stress development in anisotropic fiber-reinforced polymer composites and investigated the temperatures below the glass transition temperature of the resin. By applying two independent experimental methodologies, it was found that the initial thermal (residual) strain in the reinforcing fibers is compressive of about− 0.04% at ambient temperatures. This is due to the mismatch of the thermal expansion coefficient between the polymer matrix and fiber, as the material is cooled down from the processing temperature. However, on reheating the composites, the compressive stress in the fiber gradually diminishes and becomes zero at 50 °C. Further heating to 100 °C introduces tensile strains in the fiber of maximum of 0.13%. The conformity of these results to analytical models that relate the composite thermal strain to the thermal expansion coefficients of fiber and resin, as well as, the fiber volume fraction, is examined. Finally, the possibility of tailoring the sign (positive, negative or, even, zero) of the composite thermal expansion coefficient of certain advanced composites by simply varying the thermal expansion of the polymer matrix, is discussed.

The aim of this investigation is to define the effects of salt concentration ratio on the thermal stress and strain concentration in the exhaust tube model supposed to be made from composite material and distribution of temperature on it with time. The study build three dimensional model of exhaust tube and analyses it numerically to describe the effect of the salty environment of that exhaust tube model for two reasons the first one is the properties of composite material provide good resistance to salty and second they give a good thermal insulation.

This study has agreement with **Hilal. M. Abdullah 2011** in the effect of salt concentration on improvement the mechanical properties of composite materials.

## EXPERIMENTAL PROPERTIES OF COMPOSITE MATERIAL

The composite material is made up of polyester resin reinforced with one layer of random chopped fiber glass. The properties of resin and fiber glass are given in Table 1. (**Hansmann H**.,**2003)**.The tensile specimens were prepared by adding the curing (hardener) in ratio equal to (0.1%) and the volume fracture of the composite material specimens equals ($v_f$ =0.30).

The mechanical properties of composite material are limited by thermal conductivity test and tensile tests were made on different types of composite material according to D412 ASTM [8] as shown in Fig.1 of specimens immersed in different concentrations of salt ratio of (15%, 35% and 55%) for (40) days . The tensile tests speed was equal to (8 mm/min). The effect of salt concentration ratio on the mechanical properties such as elastic modulus and yield stress is shown in Fig.2 and Fig.3.

The preparing process of thermal conductivity specimens involves making the layer of composite material in dimensions of (200 mm* 200 mm) and then cutting that layer by using circular cutter into many smaller specimens. The experimental results show increasing thermal conductivity caused by the salt environment to be equal to (0.55 w/m.C$^o$) .

## DESIGN AND MODELING

The three-dimensional model was built of composite material of exhaust tube as shown Fig.5 The three dimensional model was built using AUTO CAD software and linked to ANSYS software for analysis for limited experimental properties which were determined from experimental test. The element type (Solid 87) [9] was used for determining the thermal distribution temperature model. The element is applicable to a 3-D, steady-state or transient thermal analysis So that, the model containing this element is also to be analyzed structurally.

## NUMERICAL ANALYSIS:

In this investigation, the finite element analysis (FEA) approach is used to perform static analysis and to obtain steady state thermal stresses from the imposed nodal temperatures (the steady state temperature distribution) obtained from thermal analysis of exhaust tube model **(Chakrapani Basavaraju, 2004**.)

The basic thermal equilibrium equation for steady state heat transfer by conduction is as follows:

$$[K^t] \{T\} = \{Q\} \quad (1)$$

where $[K^t]$ is thermal conductivity matrix; {Q} is heat flow vector; and {T} is nodal temperature vector. Shape functions *Ni* are used for interpolation of temperature inside a finite element:

$$T=[N]\{T\} \tag{2}$$

$$[N] = [\,N1 \;\; N2 \;\; \ldots..] \tag{3}$$

$$\{T\}= \{T1 \;\; T2 \;\; \ldots..] \tag{4}$$

Differentiation of the temperature- interpolation gives the following interpolation relation for temperature gradients:

$$\begin{Bmatrix} \frac{\partial T}{\partial x} \\ \frac{\partial T}{\partial y} \\ \frac{\partial T}{\partial z} \end{Bmatrix} = \begin{bmatrix} \frac{\partial N_1}{\partial x} \\ \frac{\partial N_2}{\partial y} \\ \frac{\partial N_3}{\partial z} \end{bmatrix} \{T\} = [B]\{T\} \tag{5}$$

For steady state conduction, Fourier's law for heat transfer is used **(Chakrapani Basavaraju, 2004)**,

$$q_x = - K A\, dT/dx \tag{6}$$

$$q_y = - K A\, dT/dy \tag{7}$$

$$q_z = - K A\, dT/dz \tag{8}$$

where q is the rate of heat conduction; K is the coefficient of thermal conductivity; A is the area of section which is normal to the direction of heat flow, –dT/dx, –dT/dy and –dT/dz are the temperature gradient.
The finite element equation for heat transfer is as follows:

$$\{q\}= - K [B] \{T\} \tag{9}$$

## THEORTICAL FRAMEWORK

### Steady state thermal stresses

The most common type of anisotropic material is one in which shear stresses, acting in all three reference planes, cause no normal strains (**Edward L. Wilson, 2005)**. This type of material property is very common. For example, rocks, concrete, wood, and many fiber reinforced material exhibit orthotropic behavior. For this case the equation be as the follow:

$$\begin{bmatrix} \varepsilon_1 \\ \varepsilon_2 \\ \varepsilon_3 \\ \gamma_{21} \\ \gamma_{31} \\ \gamma_{23} \end{bmatrix} = \begin{bmatrix} \frac{1}{E_1} & -\frac{\nu_{12}}{E_2} & -\frac{\nu_{13}}{E_3} & 0 & 0 & 0 \\ -\frac{\nu_{21}}{E_1} & \frac{1}{E_2} & -\frac{\nu_{23}}{E_3} & 0 & 0 & 0 \\ -\frac{\nu_{31}}{E_1} & -\frac{\nu_{32}}{E_2} & \frac{1}{E_3} & 0 & 0 & 0 \\ 0 & 0 & 0 & \frac{1}{G_4} & 0 & 0 \\ 0 & 0 & 0 & 0 & \frac{1}{G_5} & 0 \\ 0 & 0 & 0 & 0 & 0 & \frac{1}{G_6} \end{bmatrix} \begin{bmatrix} \sigma_1 \\ \sigma_2 \\ \sigma_3 \\ \tau_{21} \\ \tau_{31} \\ \tau_{23} \end{bmatrix} + \Delta T \begin{bmatrix} \alpha_1 \\ \alpha_2 \\ \alpha_3 \\ 0 \\ 0 \\ 0 \end{bmatrix} \qquad (10)$$

The study assume a constant thermal expansion i.e. ($\alpha=\alpha_1=\alpha_2=\alpha_3$) of composite material. It appears that the compliance matrix has three independent material constants. It can easily be shown that the application of a pure shear stress should result in pure tension and compression strains on the element if it is rotated 45 degrees. Using this restriction, it can be shown that (**Edward L. Wilson, 2005)**:

$$G = \frac{E}{2(1+\upsilon)} \qquad (11)$$

Therefore, for isotropic materials only Young's modulus *E* and Poisson's ratio $\upsilon$ need to be defined. The Young's modulus *E* changes with different salt concentration ratios.

The theoretical analysis of exhaust tube model is focused on determining the maximum thermal stress and strain equation (4 and 5) by depend on mechanical and thermal properties of composite material which are proposed this investigation to make the exhaust tube model.

Increase in the temperature of exhaust tube model which is fixed at each end that creates the thermal stress at its end due to thermal extension.

The total strain taking into count the effect of thermal strain which is create due to change the temperature ($\Delta$T) at cylindrical thin cylindrical pressure vessels as follows **(Clemens Kaminski, 2005):**

$$\varepsilon_T = \frac{\sigma_L}{E} - \nu \frac{\sigma_C}{E} + \alpha \, \Delta T \qquad (12)$$

where $\sigma_L$ and $\sigma_C$ are described as follows:

$$\sigma_L = PD/4t \qquad (13)$$

$$\sigma_c = PD/2t \qquad (14)$$

where

$\sigma_L$ : Longitudinal stress (MPa)

$\sigma_C$ : Circumference stress (MPa)

t :Thickness (mm)

D : Diameter of cylindrical (mm)

where (α) is thermal expansion (1/C$^o$), (ΔT) is the temperature change (C$^o$).
Maximum thermal stress is possible on surface (e.g. thin plate) where the internal pressure is (p> 0) is **(Clemens Kaminski, 2005)**:

$$\sigma_{\max} = \frac{E\alpha}{1-v}(T_i - T_f) \qquad (15)$$

And , ε=σ/E

$$\varepsilon_{\max} = \frac{\alpha}{1-v}(T_i - T_f) \qquad (16)$$

E : Young's modulus [Pa], α: linear thermal expansion coeff. [°C$^{-1}$] and *v* : Poisson's ratio [unitless].
According to this investigation which is focused on investigating the effect of thermal stress and strain, it is assumed that the internal pressure (p) in exhaust tube model is equal to zero (p=0) , so equation(3) will be as follows:

$$\varepsilon_T = \varepsilon_{ther.} = \alpha \,.\, \Delta T \qquad (17)$$

Since stress/strain = modulus of elasticity (E) then induced stress is,

$$\sigma_{ther.} = E \,.\, \alpha.\, \Delta T \qquad (18)$$

Depending on Tresca yield criterion, the yielding stress can be derived as follows **(Saduh Singh, 1990)**:

$$(\sigma_1 - \sigma_2) + (\sigma_1 - \sigma_3) + (\sigma_2 - \sigma_3) = 2k \qquad (19)$$

The value of *k* can be obtained from a simple experiment. For example, in a tension test, $\sigma_1 = \sigma_o$, $\sigma_2 = \sigma_3 = 0$ , and failure occurs when $\sigma_o$ reaches *Y*, the yield stress in tension. It follows that

$$k = \frac{Y}{2} \qquad (20)$$

In a shear test, $\sigma_1 = \tau$, $\sigma_2 = 0$, $\sigma_3 = -\tau$, and failure occurs when (τ) reaches $\tau_y$ , the yield stress of a material in pure shear,

$$k = \tau_y \qquad (21)$$

## RESULTS AND DISCUSSION

Figs. (5, 6, 7, 8, 9, 10, 11,12 and 13) show the concentration of maximum principal thermal stresses ($\sigma_x$, $\sigma_y$ and $\sigma_z$ ) at temperature (100 C$^o$) which increases by approximate ratio of (58.2% ,44.7% and 56.3%) respectively due to increase in the salt concentration ratio from (15%) to (55%). Figs.(14, 15 and 16) show the maximum thermal shear stress ($\tau_{xy}$,) at temperature of (100 C$^o$) which increase by approximate ratio of (57.17%) as a result of increase in the salt concentration ratio from (15%) to (55%). Figs.( 17, 18 and 19) show the maximum thermal shear strain ($\gamma_{xy}$) increase by ratio (21.8%) due to increase in the salt concentration ratio from (15%) to (55%).

The variation happen in principal thermal stress, thermal shear stress and thermal shear strain is caused by the effect of salty environment concentration on elastic modulus of composite material as shown in Fig. 2. The salt concentration ratio when it changes from 15% to 35% gives more effect on thermal stress and strain if compared with the effect of its increase from 35% to 55% that is caused by reaching the composite material to saturation with particles of salt which means the composite material structure refuses any more salt particles, therefore the effect is less in the interval 35% to 55% .

Figs .20 and 21 show a comparison between the theoretical and numerical results of the maximum thermal stress and strain at different salt concentration ratios. Tables 2 and 3 show the effects of salt ratio on the maximum thermal stress and stain values and nodes in which there is the concentration of maximum thermal stress Fig.22.

Figs.23, 24, 25 and 26 show the heat transition in composite exhaust tube after being attached for (180 sec) of turning the car (at external air velocity equal to zero) and the distribution of temperature with time on the body of composite exhaust tube. The study assumes time 180 sec which is required reaching the equivalence between the internal surface temperature and internal hot exhaust air temperature. The external air velocity equals zero that means no cooling occurs during 180 sec therefore after that 180 sec the external velocity of air absolutely is greater than zero and the temperature is less than shown in the analysis. The temperature of composite exhaust tube at the internal surface ranged from (83.6 $C^o$ to 109.5 $C^o$) while at the external surface is limited to the ranged from (31 $C^o$ to 50 $C^o$) which means it has a good insulation.

The experimental results show increasing thermal conductivity increase with approximate ratio (54.5%) caused by increasing the salt concentration ratio from (0 % to 55%) be equal to (0.55 w/m.$C^o$).

## CONCLUSIONS

The concentration of maximum thermal stress and strain of composite exhaust tube model is described at temperature (100 $C^o$) in different salt concentration ratios by depending on experimental results of tensile test and thermal conductivity tests. The increase in salt instruction ratio from 15% to 55% increases the thermal stress, thermal shear stress and thermal shear strain caused by increasing elastic modulus.

The concentration of maximum principal thermal stresses ( $\sigma_{x,}$ $\sigma_y$ and $\sigma_z$ ) at temperature (100 $C^o$) increases by approximate ratios of (58.2% ,44.7% and 56.3%) respectively , so that the maximum thermal shear stress ($\tau_{xy,}$) increases by approximate ratio of (57.17%) as a result of increasing the salt concentration ratio from (15%) to (55%).

The analysis model provides accurate distribution of temperature with time in the exhaust tube model showing that composite material in application field can be applied. The concentration of maximum thermal stress and strain is near the end of composite exhaust tube. The decrease in ratio between the internal and external temperature in exhaust model means that type of material gives a good insulation. The theoretical and numerical results of this research are compared with well established analytical model that relates the composite thermal strain and stress to the thermal expansion coefficient of composite mode.

**Table 1. The properties of fiberglass reinforced polyester composite**

| | Glass content wt% | Density g/cm$^3$ | | Flexural strength MPa | Flexural modulus GPa | Tensile strength MPa | Tensile modulus GPa |
|---|---|---|---|---|---|---|---|
| Chopped –stand random mat | 30 | 1.5-1.7 | | 110-190 | 6.9-8.3 | 60-120 | 6-12 |
| | | Elongation % | Compressive strength MPa | Impact strength J/mm | Thermal conductivity W/m.k | Specific heat kJ/kg.K | Coefficient of thermal expansion $10^{-6}$/K |
| | | 1-1.2 | 100-170 | 0.2-0.64 | 0.2-0.25 | 1.3-1.4 | 20-35 |

**Table 2. The effects of salt ratio on maximum values of thermal stress (σx)**

| The maximum thermal $\sigma_x$ at 15% salt ratio | | | | | | |
|---|---|---|---|---|---|---|
| NODE | 2873 | 18557 | 20600 | 1216 | 20 | 28 |
| VALUE | 0.43075E+08 | 0.19882E+08 | 0.51099E+08 | 0.49565E+08 | 0.61541E+08 | 0.81505E+08 |
| **The maximum thermal $\sigma_x$ at 35% salt ratio** | | | | | | |
| NODE | 22605 | 18557 | 20600 | 63 | 20 | 28 |
| VALUE | 0.10192E+09 | 0.44847E+08 | 0.11519E+09 | 0.14849E+09 | 0.13873E+09 | 0.18373E+09 |
| **The maximum thermal $\sigma_x$ at 55% salt ratio** | | | | | | |
| NODE | 22605 | 18557 | 20600 | 63 | 20 | 28 |
| VALUE | 0.10316E+09 | 0.45392E+08 | 0.11659E+09 | 0.15029E+09 | 0.14042E+09 | 0.18597E+09 |

**Table 3. The effects of salt ratio on maximum values of thermal shear stress (τxy)**

| The maximum thermal $\tau_{xy}$ at 15% salt ratio | | | | | | |
|---|---|---|---|---|---|---|
| NODE | 2873 | 18557 | 20600 | 1216 | 20 | 28 |
| VALUE | 0.43075E+08 | 0.19882E+08 | 0.51099E+08 | 0.49565E+08 | 0.61541E+08 | 0.81505E+08 |
| **The maximum thermal $\tau_{xy}$ at 35% salt ratio** | | | | | | |
| NODE | 22605 | 18557 | 20600 | 63 | 20 | 28 |
| VALUE | 0.10192E+09 | 0.44847E+08 | 0.11519E+09 | 0.14849E+09 | 0.13873E+09 | 0.18373E+09 |
| **The maximum thermal $\tau_{xy}$ at 55% salt ratio** | | | | | | |
| NODE | 22605 | 18557 | 20600 | 63 | 20 | 28 |
| VALUE | 0.10316E+09 | 0.45392E+08 | 0.11659E+09 | 0.15029E+09 | 0.14042E+09 | 0.18597E+09 |

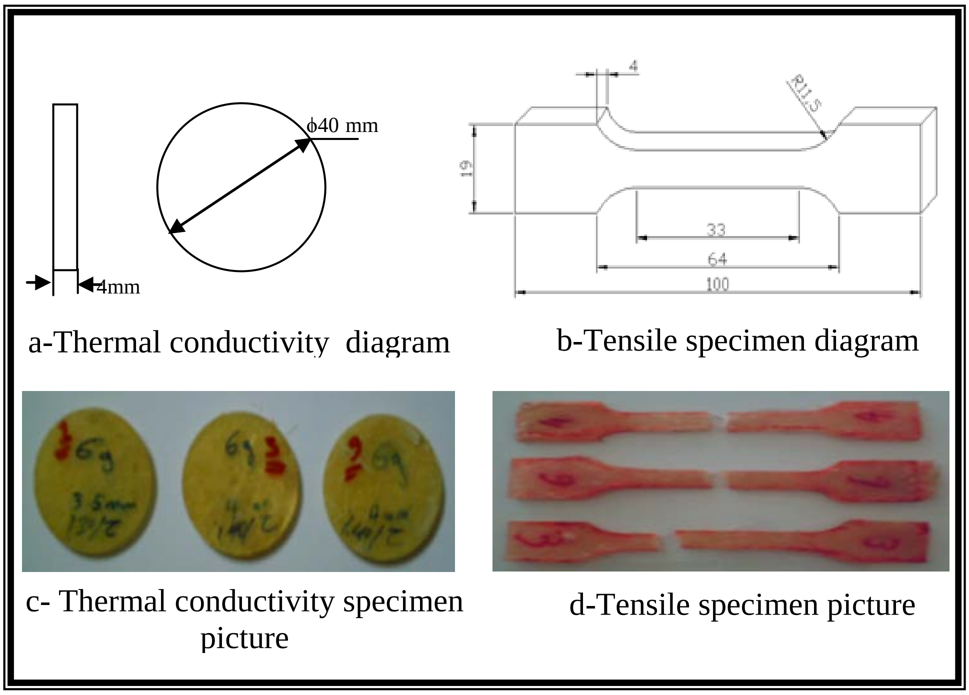


**Fig. 1-a,b,c and d . The standard thermal conductivity test and tensile test specimen [7].**

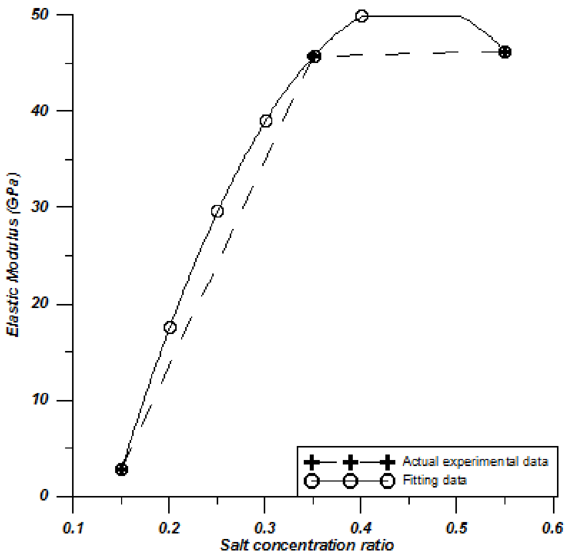


**Fig. 2 . The experimental results showing the effect of salt concentration ratio on Young's Modulus**

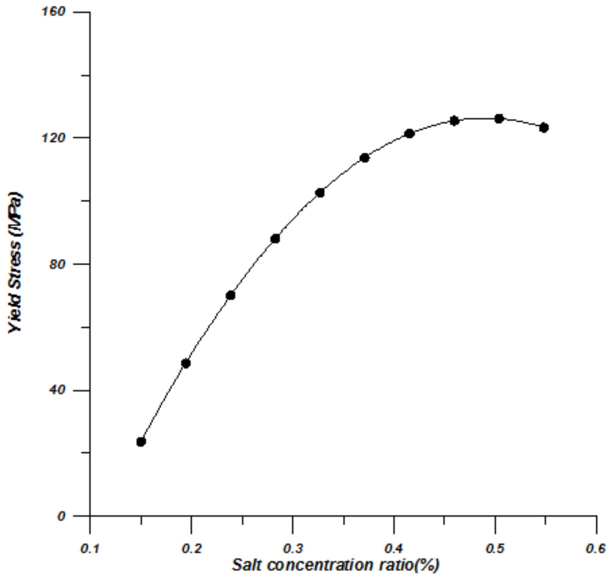


**Fig. 3 . The experimental results showing the effect of salt concentration ratio on yield stress**

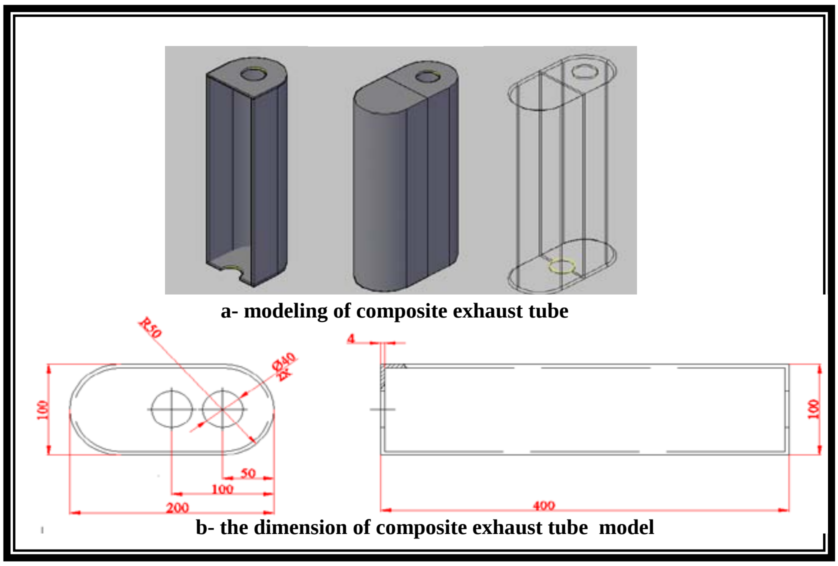


a- modeling of composite exhaust tube

b- the dimension of composite exhaust tube model

**Fig .4-a, b . AutoCAD modeling and dimensions of composite exhaust tube of car**

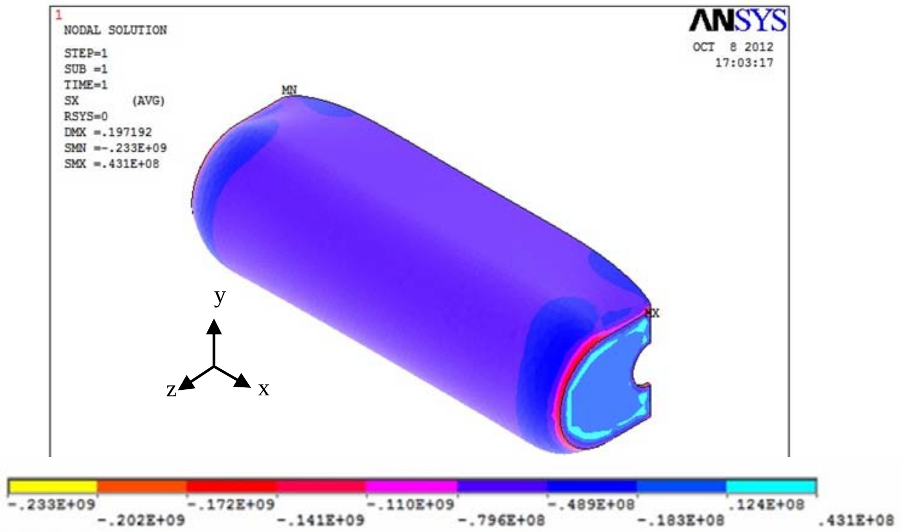


**Fig.5. Thermal stress in x-axis direction ($\sigma_x$) of composite exhaust tube in salt concentration of 15% and T=100 C$^o$**

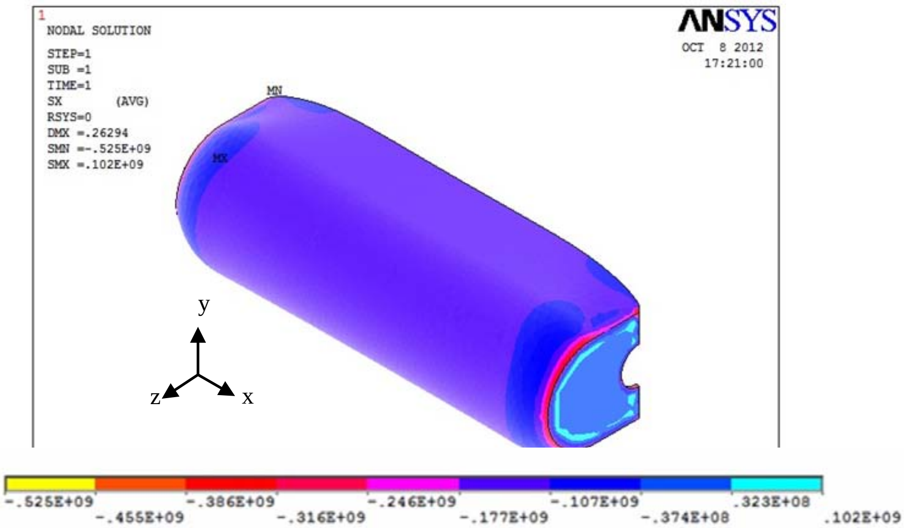


**Fig. 6. Thermal stress in x-axis direction ($\sigma_x$) of composite exhaust tube in salt concentration of 35% and T=100 C$^o$**

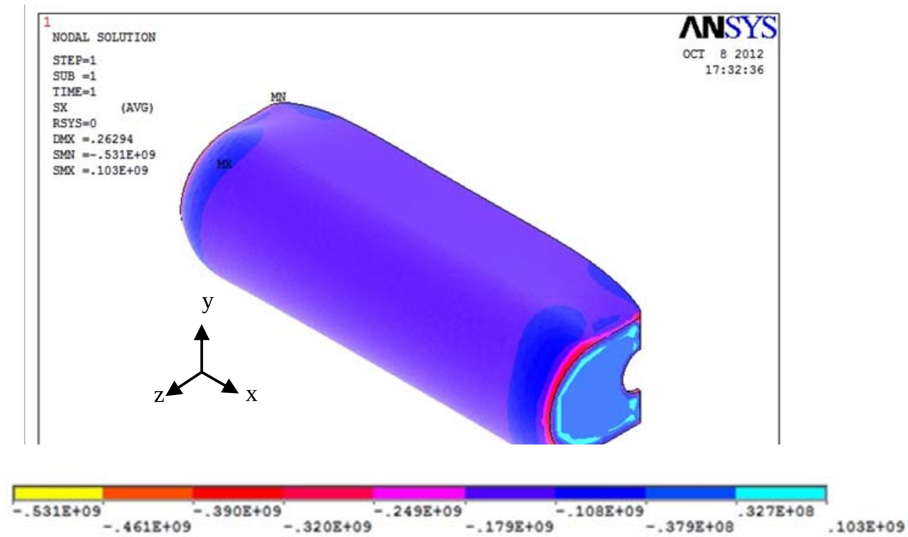


**Fig. 7. Thermal stress in x-axis direction ($\sigma_x$) of composite exhaust tube in salt concentration of 55% and T=100 C$^o$**

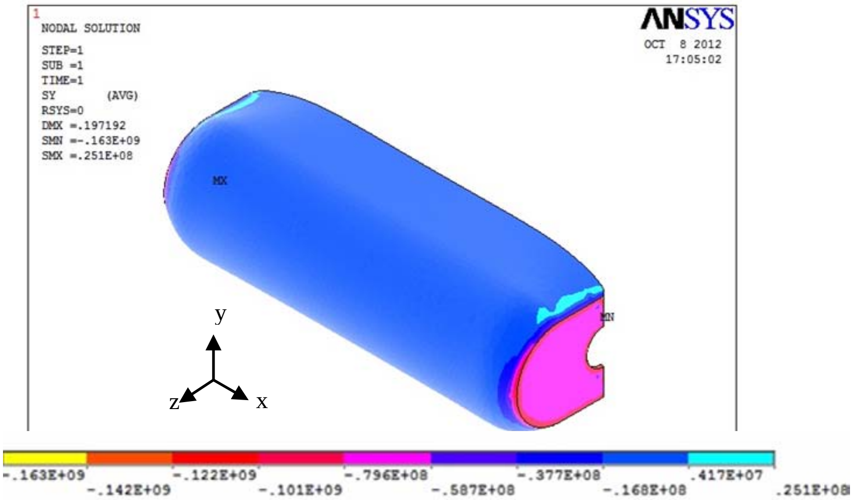


**Fig. 8. Thermal stress in y-axis direction ($\sigma_y$) of composite exhaust tube in salt concentration of 15% and T=100 C$^o$**

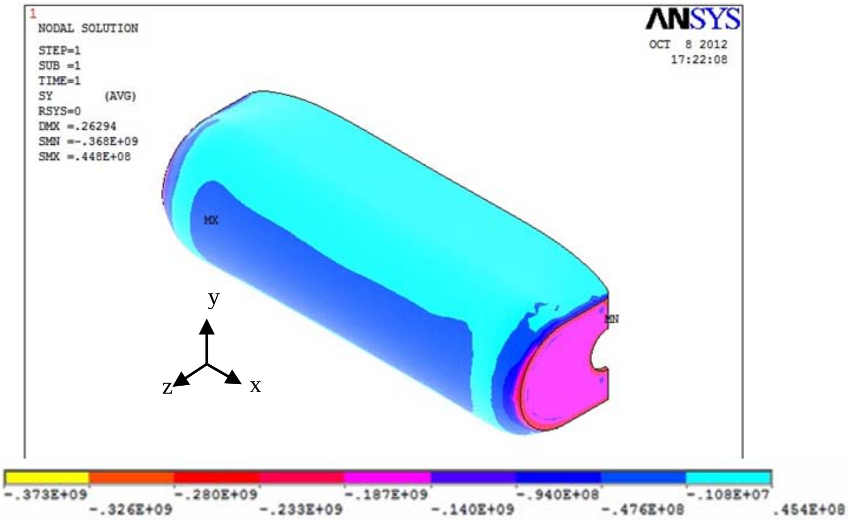


**Fig. 9. Thermal stress in y-axis direction ($\sigma_y$) of composite exhaust tube in salt concentration of 35% and T=100 C$^o$**

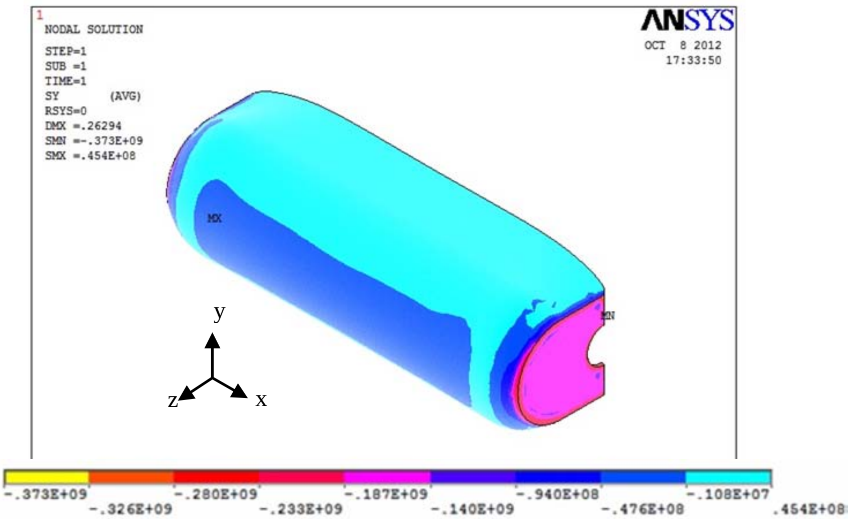


**Fig.10. Thermal stress in y-axis direction ($\sigma_y$) of composite exhaust tube in salt concentration of 55% and T=100 C$^o$**

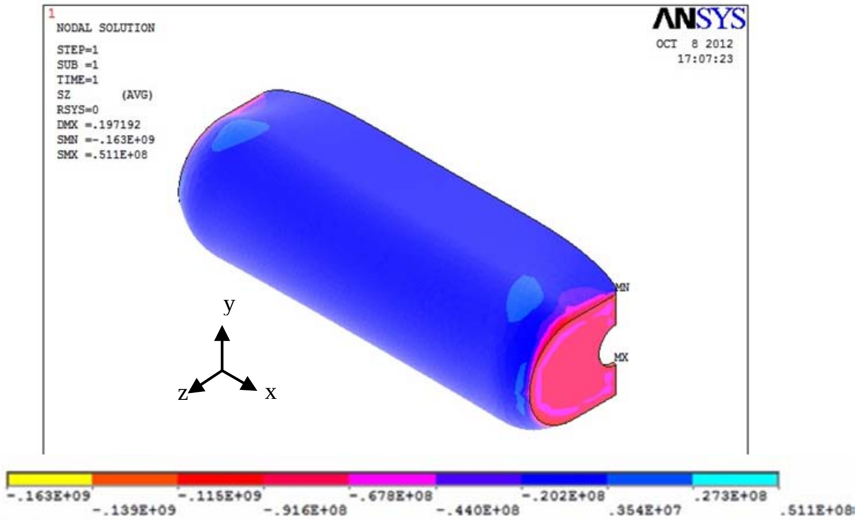


**Fig. 11. Thermal stress in z-axis direction ($\sigma_z$) of composite exhaust tube in salt concentration of 15% and T=100 C$^o$**

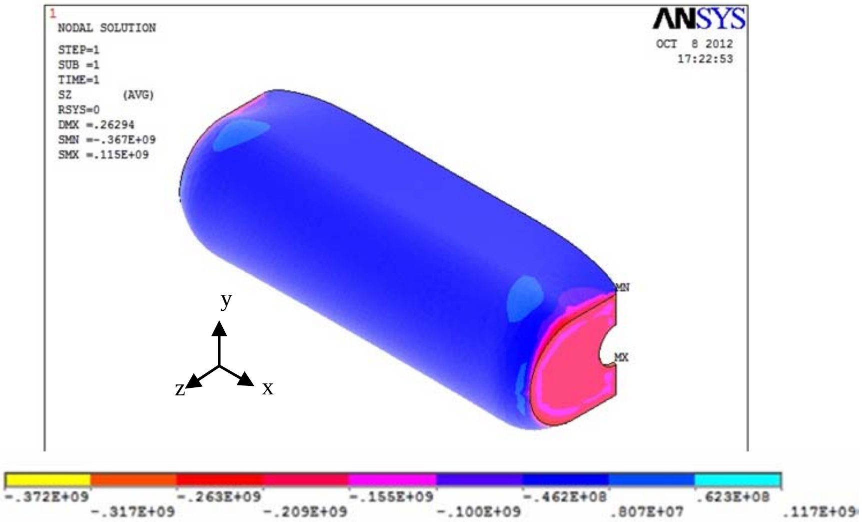


**Fig. 12. Thermal stress in z-axis direction ($\sigma_z$) of composite exhaust tube in salt concentration of 35% and T=100 C$^o$**

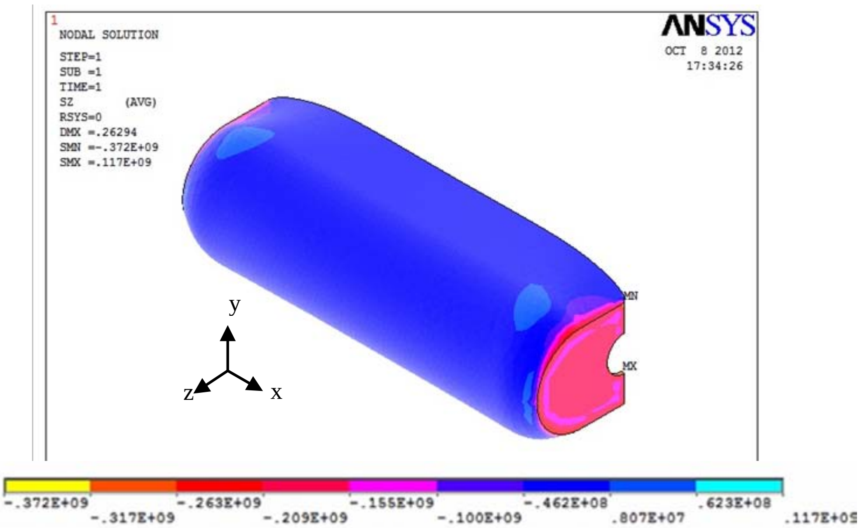


**Fig. 13. Thermal stress in z-axis direction ($\sigma_z$) of composite exhaust tube in salt concentration of 55% and T=100 C$^o$**

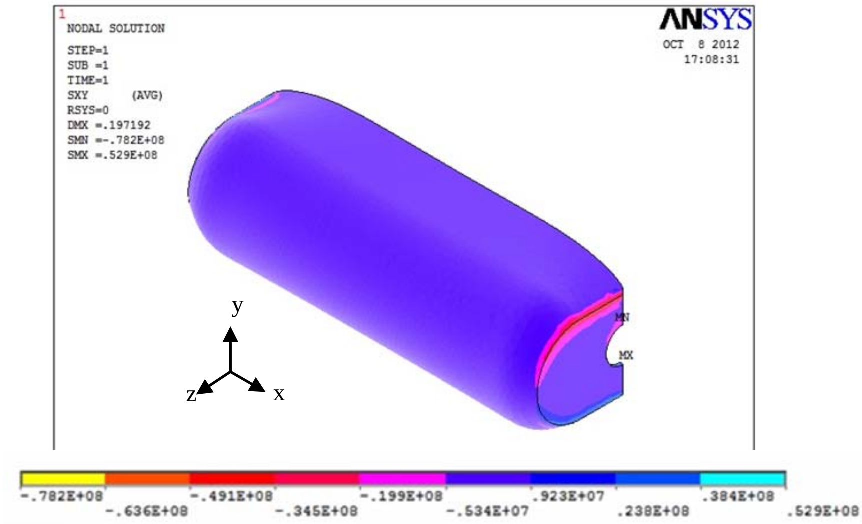


**Fig. 14. Thermal shear stress ($\tau_{xy}$) of composite exhaust tube in salt concentration of 15% and T=100 C$^o$**

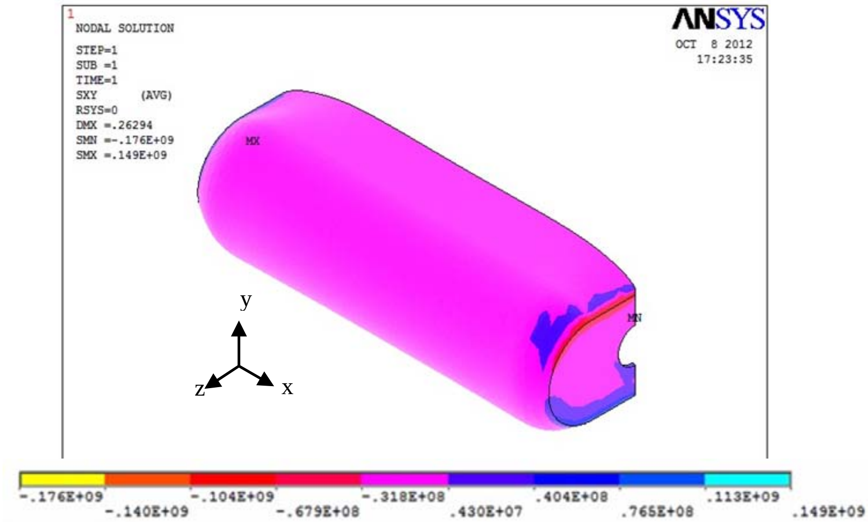


**Fig. 15. Thermal shear stress ($\tau_{xy}$) of composite exhaust tube in salt concentration of 35% and T=100 C$^o$**

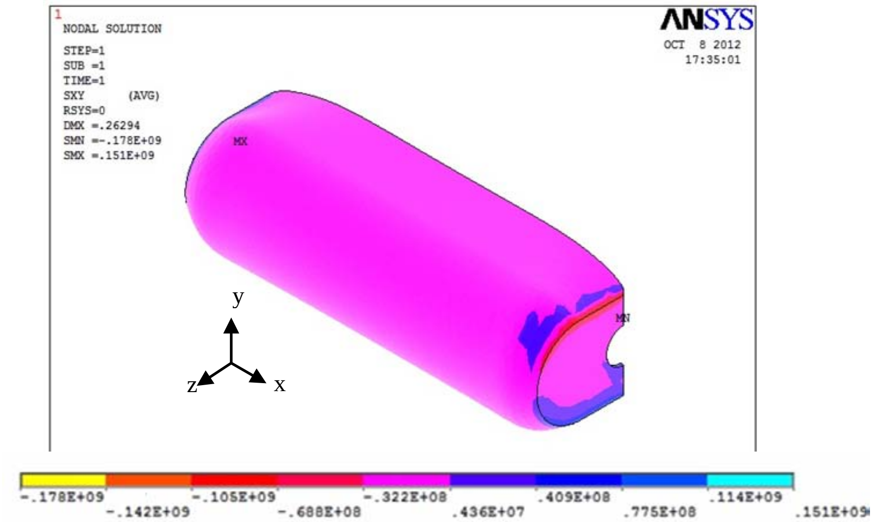


**Fig. 16. Thermal shear stress ($\tau_{xy}$) of composite exhaust tube in salt concentration of 55% and T=100 C$^o$**

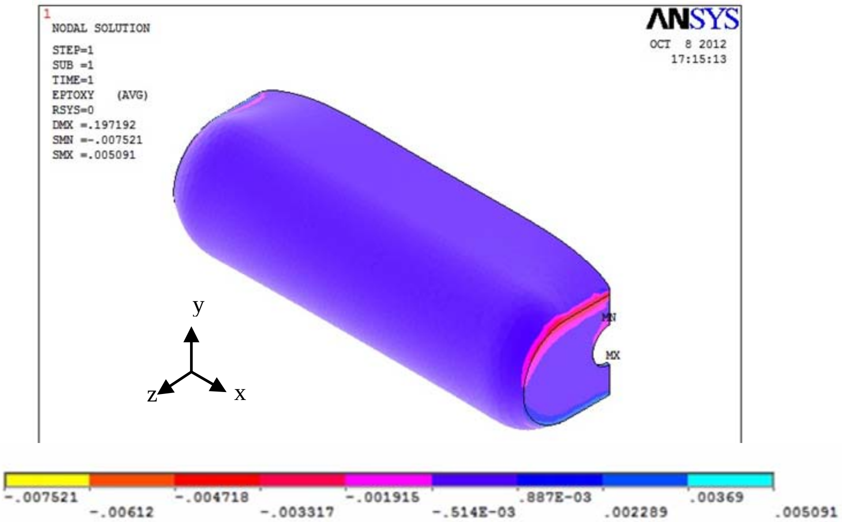


**Fig. 17. Thermal shear strain ($\gamma_{xy}$) of composite exhaust tube in salt concentration of 15% and T=100 C$^o$**

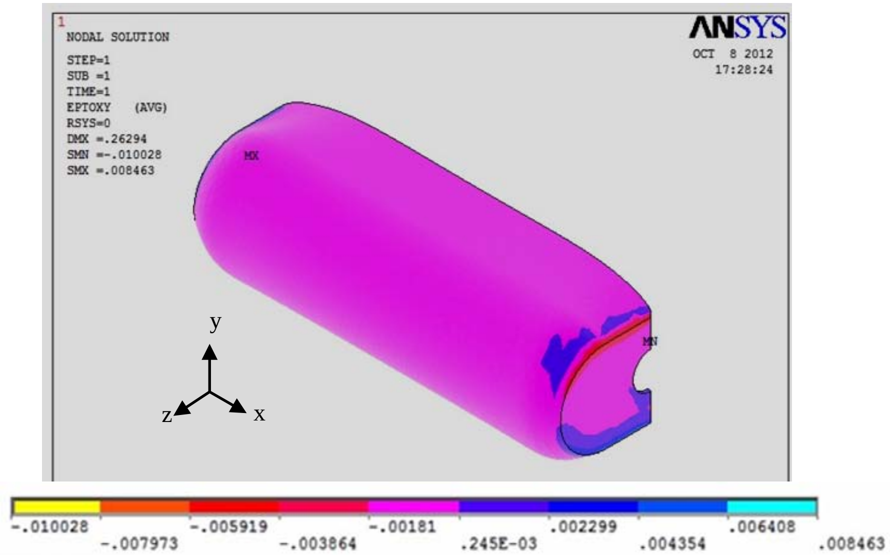


**Fig. 18. Thermal shear strain ($\gamma_{xy}$) of composite exhaust tube in salt concentration of 35% and T=100 C$^o$**

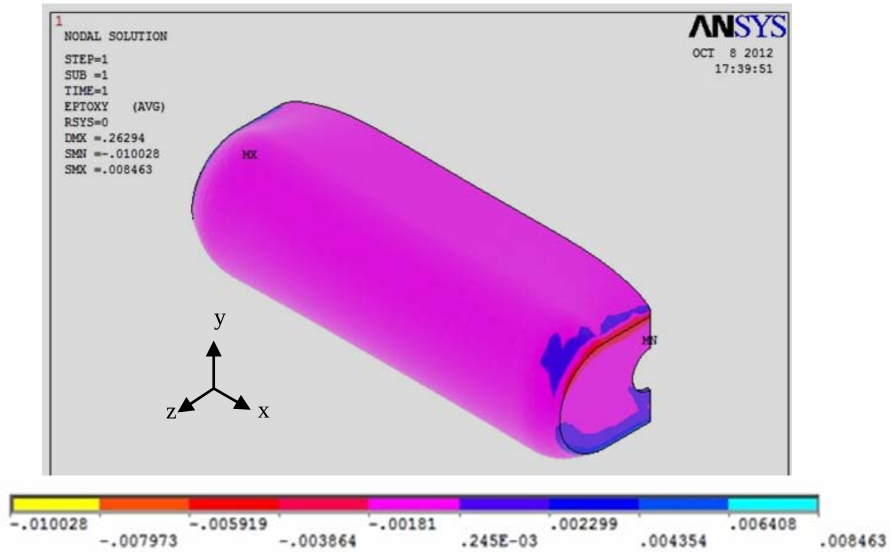


**Fig. 19. Thermal shear strain ($\gamma_{xy}$) of composite exhaust tube in salt concentration of 55% and T=100 C$^o$**

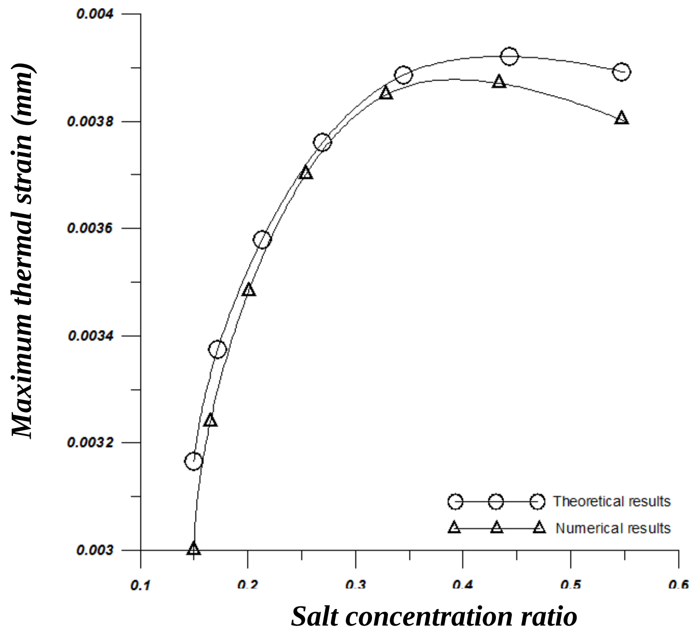


**Fig. 20. The comparison between the theoretical and numerical maximum thermal strains**

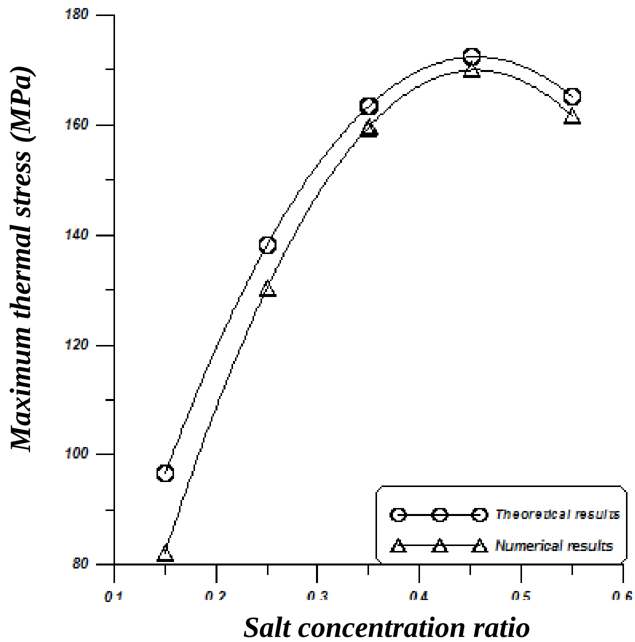


**Fig. 21. The comparison between the theoretical and numerical maximum thermal stresses**

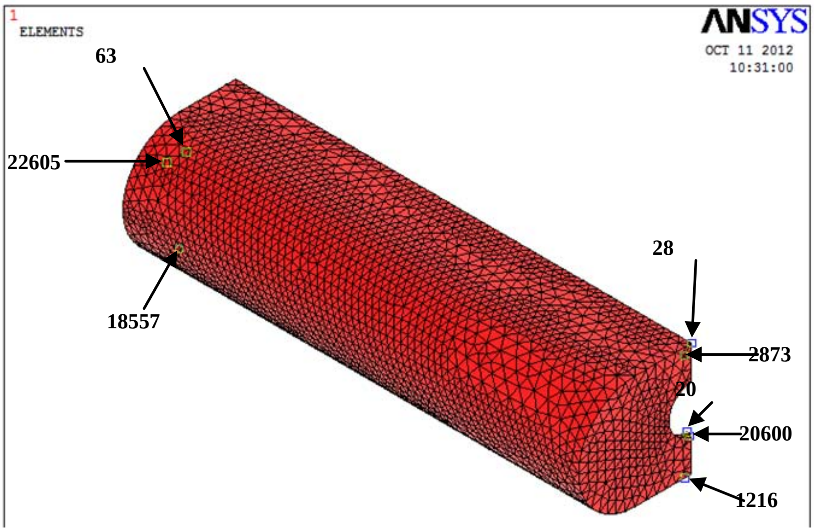


Fig. 22. The locations of nodes in Tables (2 and 3) on composite exhaust tube model

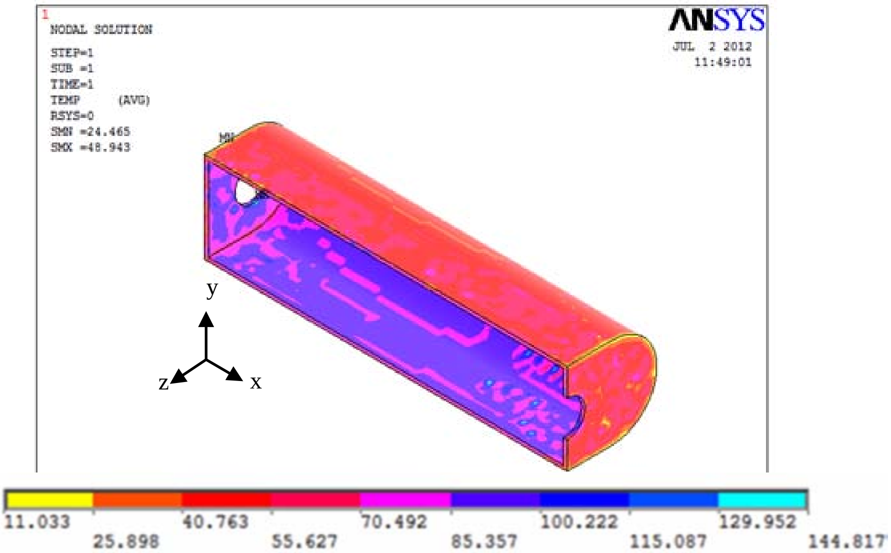


Fig. 23. The temperature distribution of composite exhaust tube of car at time of (1 sec)

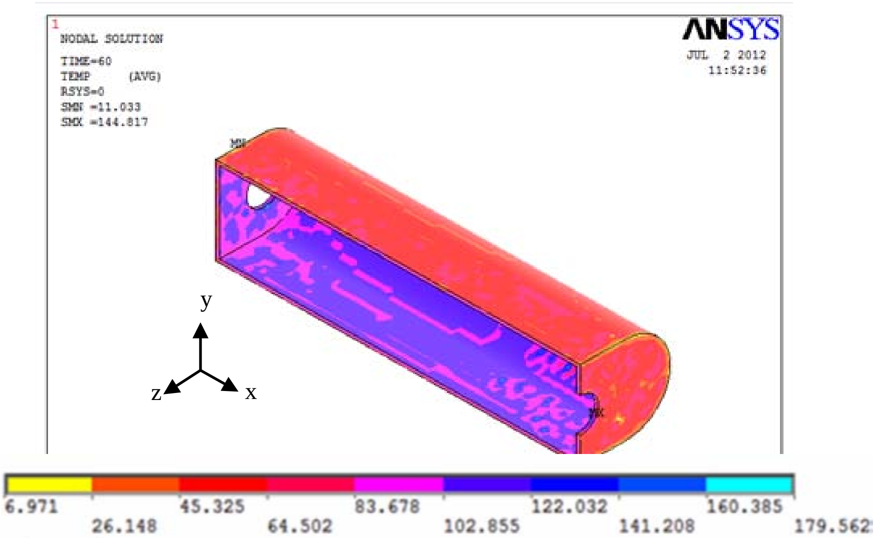


Fig. 24. The temperature distribution of composite exhaust tube of car at time of (60 sec)

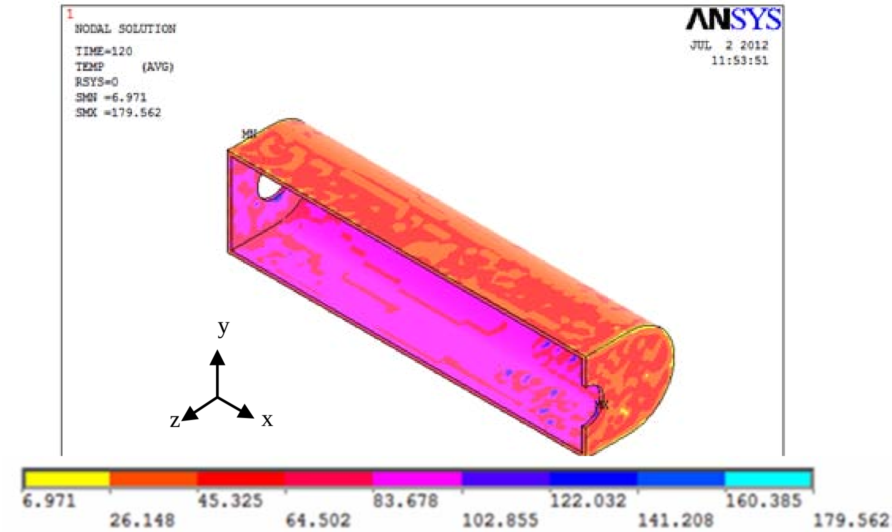


**Fig. 25. The temperature distribution of composite exhaust tube of car at time of (120 sec)**

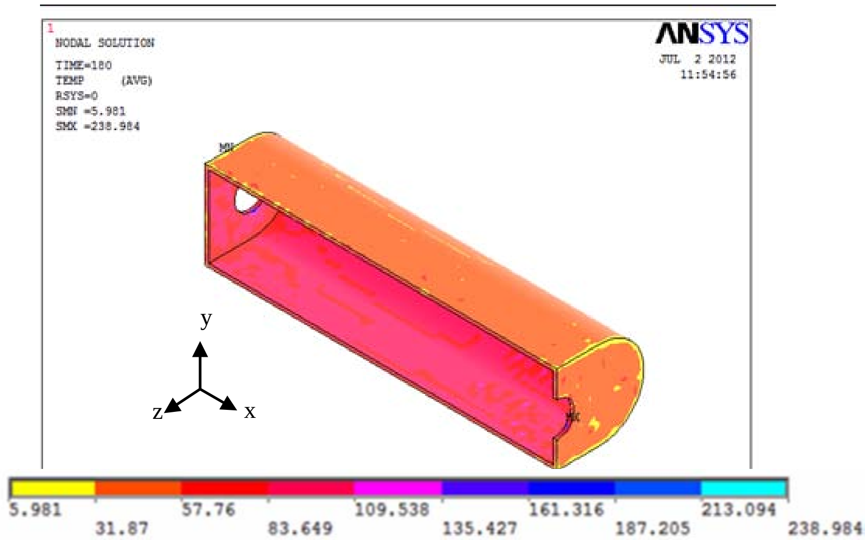


**Fig. 26. The temperature distribution of composite exhaust tube of car at time of (180 sec)**

## REFRENCES :-


- Abdalla A. Ab. Rashdi, Mohd Sapuan Salit, Khalina Abdan and Megat Mohamad Hamdan Megat, " Water Absorption Behaviour of Kenaf Reinforced Unsaturated Polyester Composites and Its Influence on Their Mechanical Properties", Pertanika J. Sci. & Technol. 18 (2), 433 – 440 , 2010.

- Anagnostopoulos G., Parthenios J. and Galiotis C. ," Thermal Stress Development in Fibrous Composites", Materials Letters Vol.62, pp 341–345, 2007.

- Chakrapani Basavaraju, " Thermal Stresses At Dissimilar Pipe-Stanchion Interfaces", ASME Pressure Vessels and Piping Conference , 2004.

- Clemens Kaminski**,** "Stress Analysis and Pressure Vessel", Lent Term 2005**.**

- Edward L. Wilson, " Three-Dimensional Static and Dynamic Analysis of Sttructures",Third Edition, January 2005.

- Eyassu Woldesenbet, Nikhil Gupta**, "**Determination of Moisture Effects on Impact Properties of Composite Materials", Journal of Material Science, Vol. 37, No. 13, pp. 2693-2698,2004.

- Hansmann H. " Composite ASM Handbook", 2003.

- Hilal. M. Abdullah " Studying the Effect of Some Inorganic Phosphors Salts on Fire Retardant and Mechanical Properties of Partially Cross Linked Modified Unsaturated polyester Composite",2011.

- Imgrund M. and Swanson C., "ANSYS® Verification Manual", Analysis Systems, Inc. (1992).

- Radoljub P. Tomi, Aleksandar S. Sedmak, Dobrivoje M. Ati, Marko V. Milos, and Zoran Stefanovi," Thermal Stress Analysis Of A Fiber-Epoxy Composite Materail",Thermal Science, , Vol. 15, No. 2, pp. 559-563, 2011.

- Saduh Singh, "Theory of Plasticity", Khana Publishers-Delhi, 1990.

- Standard Tensile Test ASTM-D412.